Kinetics of Thermal Pyridine Dissociation of Ni(*N*-arylsalicylideneaminato)$_2$-(pyridine)$_2$ in Solid Phase

Kikuo MIYOKAWA,* Hidenori HIRASHIMA, and Isao MASUDA

Department of Chemistry, Faculty of Science, Fukuoka University, Nanakuma, Nishi-ku, Fukuoka 814-01

(Received February 16, 1981)

The kinetics of the thermal pyridine dissociation reactions of Ni[*N*-(R-C_6H_4)salam]$_2$py$_2$, where R=H(**1**), *p*-F(**2**), *p*-CH_3O(**3**), *p*-CH_3(**4**), *p*-Cl(**5**), and *p*-Br(**6**), in solid phase, were analyzed by the isothermal weight-loss measurements. On pyrolysis, these pyridine adducts with an octahedral coordination geometry of Ni(II) liberated pyridine to leave products with the formula Ni[*N*-(R-C_6H_4)salam]$_2$. The product obtained from **2** was the diamagnetic monomer, those from **4**—**6** were paramagnetic polymers with μ_{eff}=(3.11—3.30) μ_B, and that from **3** was paramagnetic with an intermediary moment of μ_{eff}=1.45 μ_B. Reaction mechanisms were different depending on the nature of R: **2** followed the contracting disk equation with E =163 kJ/mol; **3**—**6** followed the contracting disk equation in the initial period of the reaction (the E_a values were 97 for **3**, 134 for **4**, 173 for **5**, and 172 kJ/mol for **6**) and then all except **3** followed Jandar's equation, in the subsequent period. These E_a values were considered to reflect the bond stability between the central Ni(II) ion and the axial pyridine ligands; these values increased with an increase in the electron-withdrawing property of R. The pyridine dissociation reaction may give rise to the complexes of the monomeric square-planar or to those of the associated, polymeric octahedral structure. Which result occurs does not depend only on the tendency of the central Ni(II) ion to accept, at the apical positions, the coordinate bond from the adjacent molecules.

Extensive investigations on bis(*N*-substituted salicylideneaminato)nickel(II) complexes have revealed that, in non-donor solvents, these complexes exist as a mixture of square-planar, tetrahedral, dimeric square-bipyramidal, and polymeric octahedral species.[1] The di- or polymeric species is thought to arise from the association of the planar species through the coordination bonding of the phenolato oxygen atoms in the complex molecule with the central Ni(II) ion of the adjacent molecules at the apical positions.[2] Thus, the association seems to be related to the Lewis base accepting ability of the central Ni(II) ion. However, the diversity of the solute species makes it difficult to evaluate the Lewis acidity of Ni(II) ions in these complexes, in solution.[3]

In order to estimate the Lewis acidity of the Ni(II) ion, the series of the complexes bis[*N*-(*p*-substituted aryl)salicylideneaminato]bis(pyridine)Ni(II), abbreviated as Ni[*N*-(R-C_6H_4)salam]$_2$py$_2$, have been subjected to a kinetic study of the thermal pyridine liberation reaction in solid phase.

Experimental

Materials. The parent complexes Ni[*N*-(R-C_6H_4)-salam]$_2$ were prepared by the published procedure.[4,5] Their bis(pyridine) adducts were isolated as previously described.[6] The adducts were identified by the nickel and pyridine analyses.

Measurements. TG and DSC curves were recorded on a Rigaku Denki Thermal Analyzer Model 8002 and isothermal weight-loss curves on a Sinku Riko micro-DTA apparatus Model TGD-3000-RH. These measurements were carried out under a constant flow of nitrogen, 100 ml/min. No influence from the variation of the nitrogen flow rate (in the range from 50 to 150 ml/min) was observed. Other physicochemical data were obtained as previously reported.[6]

Results and Discussion

The effective magnetic moments of the bis(pyridine) adducts and the products obtained after the adducts were heated up to 200 °C to eliminate pyridine, are compared with those of the parent Ni[*N*-(R-C_6H_4)-salam]$_2$ complexes in Table 1. The reflectance spectral data are also shown in Table 1. Parent complex **2**, as well as **1**, is diamagnetic, corresponding to the singlet state of Ni(II), and the spectrum exhibits an absorption maximum at 16.1×10^3 cm^{-1}; this is ascribed to the square-planar crystal field band, $^1A_{1g}\rightarrow{}^1A_{2g}$ transition of Ni(II).[7] On the other hand, the new parent complexes **3** and **6** are paramagnetic and these paramagnetisms correspond to the triplet state of Ni(II). Moreover, their spectra comprise two peaks with the maxima around 10.0 and 16.5×10^3

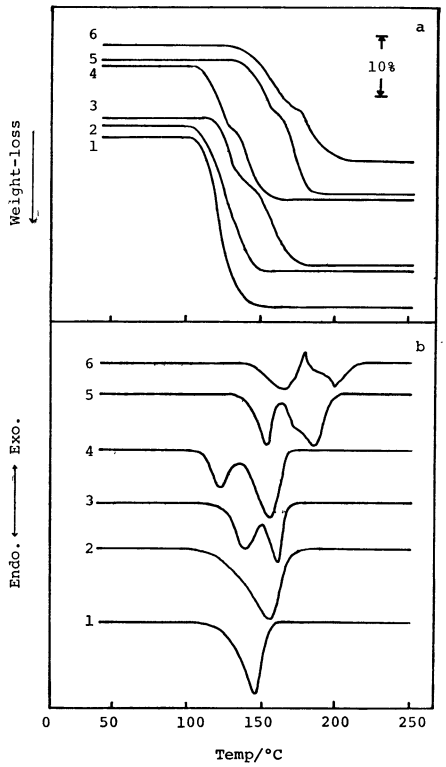

Fig. 1. TG(a) and DSC(b) curves of pyridine adducts; heating rate 10 °C/min. The numbers correspond to those given in Table 1.

Table 1. Magnetic, electronic spectral, and thermal data on the parent complexes Ni[*N*-(R-C_6H_4)salam]$_2$ and their bis(pyridine) adducts Ni[*N*-(R-C_6H_4)salam]$_2$py$_2$

No.	R	Parent complex				Bis(pyridine) adduct	Pyridine-liberated product	
		μ_{eff}[a] / μ_B		ν_{max}[b] / 10^3 cm^{-1}	t_m / °C	μ_{eff}[a] / μ_B	μ_{eff}[a] / μ_B	t_m[c] / °C
1	H	dia[d]	(dia)[e]	16.3	276	3.09 (2.9)[f]	dia	276
2	*p*-F	dia	(dia)[e]	16.1	271	3.16	dia	272
3	*p*-CH_3O	3.40		10.1, 16.5	266	3.14	1.45	264
4	*p*-CH_3	3.30	(3.28)[e]	10.3, 16.5	275	3.17	3.30	280
5	*p*-Cl	3.31	(3.34)[e]	10.2, 16.6	287	3.31	3.28	287
6	*p*-Br	3.36		10.0, 16.5	291	3.15	3.11	297

a) Effective magnetic moment. b) Powder reflectance. c) DSC-peak maximum temperature due to melting. d) dia: Diamagnetic. e) Ref. 5. f) Ref. 4.

cm^{-1}; these are respectively ascribed to the $^3A_{2g}\rightarrow{}^3T_{2g}$ and the $^3A_{2g}\rightarrow{}^3T_{1g}(F)$ transitions of Ni(II) in the octahedral crystal field.[7] The magnetic and the spectral characteristics indicate the coordination structure of the parent complexes to be square planar for **1** and **2** and octahedral for **3**—**6**.

In Fig. 1, the TG and DSC curves of the pyridine adducts are reproduced. The TG curves show that all the adducts investigated lose 2 mol of pyridine per mole of the adduct in the range (100—200) °C. Adduct **2**, like **1**,[6] shows one endothermic DSC peak and a weight-loss of 2 mol pyridine per mole of the adduct on one stage in the TG curve. But adducts **3**—**6** show two endothermic DSC peaks and, in the corresponding TG curves, they show the loss of 2 mol pyridine per mole of the adduct through two stages. Up to the break point temperature in the TG curve, the weight-loss amounts to *ca.* 40—60% of the total pyridine loss. This fact implies that in the cases of adducts **3**—**6** pyridine is liberated in two steps and hence that the formation of mono(pyridine) adduct may be expected. However, pyrolysis of these adducts at 120 °C, apparently lower than their first DSC peak temperatures, only resulted in leaving a product with the formula Ni[*N*-(R-C_6H_4)salam]$_2$. Dakternieks *et al.* have reported that the mono(pyridine) adducts of Ni(*N*-*n*-Bu-salam)$_2$ and Ni(*N*-*n*-Bu-5-Cl-salam)$_2$ are formed along with their bis(pyridine) adducts in the toluene solution containing pyridine, though the TG curves of these bis(pyridine) adducts show a smooth continuous weight-loss, indicating no evidence for the formation of a five-coordinated intermediate.[3]

As seen in Table 1, the products obtained by eliminating pyridine show either dia- or paramagnetism, in accord with the respective parent complexes, excluding product **3** which shows an intermediary magnetic moment. Product **3** is thought to be composed of both paramagnetic and diamagnetic species. It is noticed that for the diamagnetic monomeric product **1**[6] and **2**, their X-ray powder diffraction patterns were coincident with those of the respective parent complexes, while for the paramagnetic polymeric products **4**—**6**, the X-ray patterns did not agree with those of the respective parent complexes. Clark and O'Brien noted that for polymeric Ni(*N*-CH_3-5-Cl-salam)$_2$ the X-ray pattern of the sample obtained from the solution is not completely identical to that obtained by heating the monomeric modification in solid phase.[8]

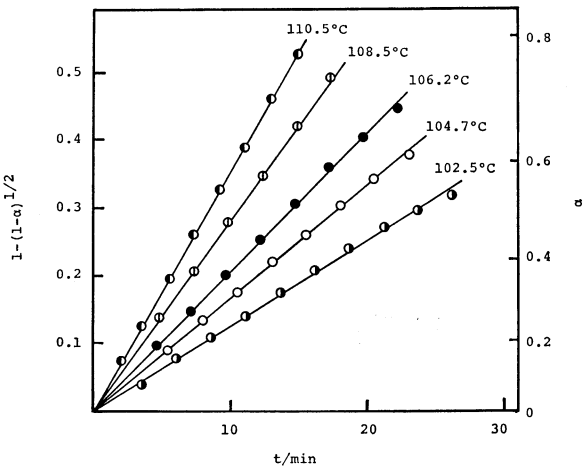

Fig. 2. Contracting disk rate plots for the pyridine liberation reaction of Ni[*N*-(*p*-F-C_6H_4)salam]$_2$py$_2$ (**2**).

The pyridine liberation process of adduct **1** has already been reported to follow the first order equation (Eq. 1) through $\alpha=0$—0.70[6]

$$-\ln(1-\alpha) = kt, \quad (1)$$

where α, k, and t are the molar fraction of the adduct which liberated pyridine, the rate constant, and the reaction time, respectively. Adduct **2** differs from **1**; its pyridine liberation process is found to fit the contracting disk equation (Eq. 2) through $\alpha=0$—0.65, as shown in Fig. 2:

$$1-(1-\alpha)^{1/2} = kt. \quad (2)$$

This fact may be interpreted by assuming that the reaction rate is determined by the reaction occurring at the phase boundary.[9]

The pyridine liberation process for adducts **3**—**6** were somewhat complicated in comparison with those for the above two cases. As is exemplified in Fig. 3 with the rate plots for **4**, the reaction mechanism appears to be altered with the progression of the pyridine dissociation reaction. The rate plots indicate

Table 2. Kinetic data of pyridine liberation reactions of Ni[*N*-(R-C_6H_4)salam]$_2$py$_2$

No.	R	α[a]	Reaction[b] scheme	$k/10^{-3}$ min^{-1} (Temp/°C)	E_a/kJ mol^{-1}
1	H[c]	0—0.70	A	6.68 (86.8), 9.37 (88.8), 12.3 (90.6), 17.3 (93.0)	167±4
2	*p*-F	0—0.65	B	12.8 (102.5), 17.0 (104.7), 20.8 (106.2), 28.2 (108.5) 38.8 (110.5)	163±4
3	*p*-CH_3O	0—0.45	B	3.06 (89.5), 3.53 (91.8), 5.30 (96.4), 7.77 (100.5)	97±5
4	*p*-CH_3	0—0.35	B	1.57 (106.8), 2.08 (110.8), 4.98 (118.5), 10.4 (124.8)	134±8
		0.35—0.75	C	0.84 (106.8), 1.75 (110.8), 3.66 (118.5), 10.1 (124.8)	159±14
5	*p*-Cl	0—0.30	B	4.17 (123.4), 5.84 (126.8), 10.8 (131.7), 20.1 (135.6)	173±12
		0.30—0.70	C	0.61 (123.4), 1.13 (126.8), 1.45 (131.7), 3.76 (135.6)	183±35
6	*p*-Br	0—0.30	B	5.00 (132.7), 5.87 (133.4), 21.7 (145.0), 30.8 (147.0)	172±7
		0.30—0.70	C	1.21 (132.7), 1.32 (133.4), 3.35 (145.0), 5.08 (147.0)	131±13

a) α: Molar fraction of the adduct liberated pyridine. b) A: $-\ln(1-\alpha)=kt$, B: $1-(1-\alpha)^{1/2}=kt$, C: $[1-(1-\alpha)^{1/3}]^2=kt$. c) Ref. 6.

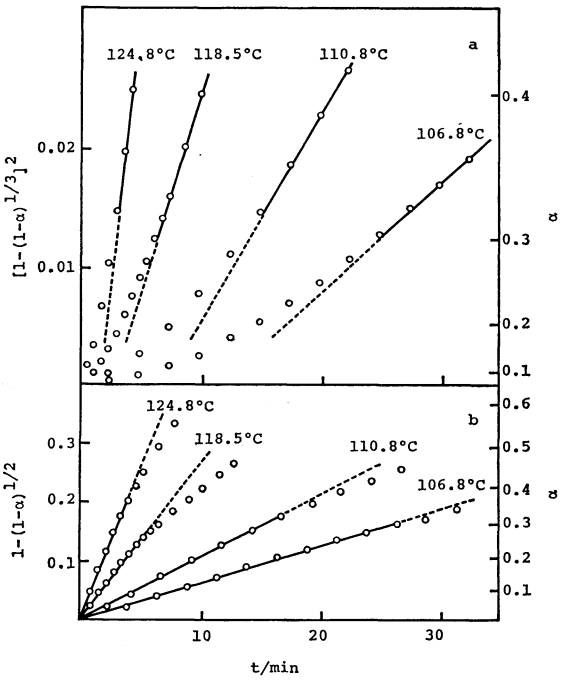

Fig. 3. Jandar's rate plots(a) and contracting disk rate plots(b) for pyridine liberation reaction of Ni[*N*-(*p*-CH_3-C_6H_4)salam]$_2$py$_2$ (**4**).

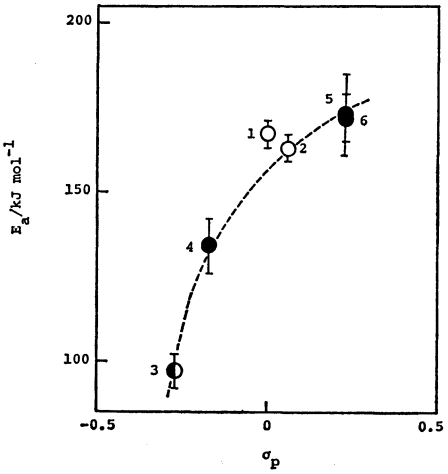

Fig. 4. Plots of activation energy, E_a *vs.* Hammett's σ_p value.
The numbers correspond to those in Tables 1 and 2.
○: Monomeric product, ●: polymeric product, ◐: (monomeric+polymeric) product.

that, in the initial period during α=0—0.35, the reaction progresses according to the contracting disk equation, as was observed for adduct **2**; however, in the subsequent period of α=0.35—0.75, it follows Jandar's equation (Eq. 3):[10]

$$[1-(1-\alpha)^{1/3}]^2 = kt. \quad (3)$$

Thus, these two processes of pyridine liberation would cause the apparent doubling observed in the TG and DSC curves of adducts **3**—**6**, as described above. The fact that the reaction follows Jandar's equation could be interpreted as meaning that the reaction is strongly influenced by the diffusion process of the liberated pyridine. For adducts **4**—**6**, which form the octahedral polymeric products upon pyrolysis, we think that as the pyridine dissociation proceeds, it becomes difficult for the free pyridine molecule to diffuse through the close product layer consisting of the polymeric species. An attempt to describe the isotherms for adduct **3** in the above subsequent period was unsuccessful.

The kinetic data are summarized in Table 2. With respect to the reactions described by Eq. 2, the values of the activation energy, E_a, are plotted against Hammett's substitution constant σ_p of R[11] in Fig. 4; the plots indicate that the E_a value increases with an increase in the electron-withdrawing property of R. As to the reaction described by Eq. 1, the E_a value does not deviate from this relation. No relation like the above was found for the reactions following Eq. 3. The electron-withdrawal through R is expected to stabilize the bonding of Ni(II) toward the axial pyridine ligands, as it may increase the Lewis acidity of the Ni(II) ion. Hence, the E_a values for the reactions following Eqs. 1 and 2 are considered to reflect mostly the bond stability between Ni(II) ion and the axial pyridine. From the solution equilibrium data on the pyridine adduct formation of Cu(*N*-R-salam)$_2$, which includes the Schiff bases with substituted aryl groups, Ewert *et al.*[12] have concluded that the electron-withdrawal by the substituent R on

the aryl ring is transmitted *via* N atom, thus decreasing the electron-density on Cu(II) ion.

Furthermore, Fig. 4 indicates that whether pyridine dissociation reaction gives rise to a square-planar monomer or to an associated octahedral polymer is not determined only by the E_a values; that is, the association of monomeric square-planar Ni(II) complexes forming the octahedral polymeric complexes is not affected solely by the Lewis acidity of the central Ni(II) ion. Though the basicity of the phenolato O atom should be taken into account in a discussion of the present association, the results of Ewert *et al.*[12] suggest that the substitution on aryl ring will exert its electronic effect on Ni(II) ion predominatly *via* N atom. Another factor would be a steric effect caused by substitution. Tsuchiya *et al.* have reported that "deaquation" of [Ni(diamine)$(H_2O)_2$]X_2 (diamine=*N*,*N*′-diethyl-, *N*,*N*′-dimethyl-, and *N*,*N*-diethylethylenediamine; X=anion) gives either octahedral [Ni(diamine)$_2X_2$] or square-planar [Ni(diamine)$_2$]X_2 depending on the steric effects arising from the *N*-substituents.[13] As far as the present complexes are concerned, the rather more bulky R seems to favor the associated form.

References

1) R. H. Holm, G. W. Everett, and A. Chakravorty, *Progr. Inorg. Chem.*, **7**, 83 (1966).
2) C. H. Harris, S. L. Lenzer, and R. L. Martin, *Aust. J. Chem.*, **11**, 331 (1958); R. H. Holm, *J. Am. Chem. Soc.*, **83**, 4683 (1961).
3) D. R. Dakternieks, D. P. Gordon, L. F. Lindoy, and G. M. Mockler, *Inorg. Chim. Acta*, **7**, 467 (1973).
4) F. Basolo and W. R. Matoush, *J. Am. Chem. Soc.*, **75**, 5663 (1953).
5) R. H. Holm and K. Swaminathan, *Inorg. Chem.*, **2**, 181 (1963).
6) K. Miyokawa, H. Hirashima, and I. Masuda, *Bull. Chem. Soc. Jpn.*, **54**, 3361 (1981).
7) A. B. P. Lever, "Inorganic Electronic Spectroscopy," Elsevier, Amsterdam (1968), p. 333.
8) H. C. Clark and J. O'Brien, *Can. J. Chem.*, **39**, 1030 (1961).
9) "Chemistry of Solid States," ed by W. E. Garner, Butterworth, London (1955), p. 184.
10) W. Jandar, *Z. Anorg. Chem.*, **163**, 1 (1927).
11) H. H. Jaffe, *Chem. Rev.*, **53**, 191 (1953).
12) A. Ewert, K. J. Wannowius, and H. Elias, *Inorg. Chem.*, **17**, 1691 (1978).
13) R. Tsuchiya, A. Uehara, A. Izumi, and S. Joba, 30th Nat. Conf. on Coordination Chemistry of Japan, Tokyo, Oct 1980, Abstr. No. 1B15.